Journal of Water Sciences Research,
ISSN: 2251-7405 eISSN: 2251-7413
Vol. 9, No. 1, Spring 2017, 37-46, JWSR

JWSR

Application of Soft Computing Methods in the Analysis of Velocity Field in Dividing Channel

Sohrab Karimi[1*], Hossein Bonakdari[2], Hojat Karami[3], Amir Hossein Zaji[4]

1. Ph.D. Student, Department of Civil Engineering, Semnan University, Semnan, Iran

2. Associate Professor, Department of Civil Engineering, Razi University, Kermanshah, Iran

3. Assistant Professor, Department of Civil Engineering, SemnanUniversity, Semnan, Iran

4. Ph. D. Student, Department of Civil Engineering, Razi University, Kermanshah, Iran

Received: 2 July 2016 Accepted: 22 October 2016

ABSTRACT

The simplest water diversion method in irrigation systems is using intakes. Measuring the mean velocity is one of the essential hydraulic parameters in increasing the efficiency of the intake. In this study, the mean velocity was predicted for different width ratios of an intake using ANN-MLP neural network model. In order to do that, the flow field within a 90-degree intake was first simulated three-dimensionally using ANSYS-CFX. The neural network used in this study includes 3 inputs; longitudinal coordinate (Y^*), ratio of the branch channel to the main channel (w_r), and mean velocity of the middle line of the channel cross section (V^*_{line}). V^*_{line} is the average velocity in the vertical column of the branch channel, which has been measured by the ANSYS-CFX model after the validation. Comparison of the ANSYS-CFX results with the experimental ones indicated that this model, with mean Root Mean Squared Error (RMSE) of 0.013, has a proper accuracy in simulating the characteristics of the flow field within the intake. In addition, comparison of the obtained results from ANN-MLP model and the experimental results indicated that this model, with mean determination coefficient (R^2) of 0.948, has a high performance in predicting the mean velocity of open channel intakes.

Keywords

Intake, mean velocity, width ratios, ANN model.

1. Introduction

Diverting water from rivers and main channels is done through the intake for the purposes such as water delivery for agricultural objectives, urban wastewater collection systems and generating energy. A completely complex flow is formed as the flow enters the branch channel from the main channel (Seyediyan et al., 1389, Shamlou et al., 1389, Safarzadeh et al., 1383 and 1387). As the flow approaches the branch channel, it undergoes transverse acceleration due to the suction pressure caused by the division and it is divided into two parts. A part of the flow enters the intake while the rest of the flow continues moving forward within the main channel (Ramamurthy et al., 2007, Issa et al., 1994, Neary et al., 1996, Shettar et al., 1996, Barkdoll et al., 1998). The flow entering the intake loses balance due to the side pressure gradient, shear stress, and centripetal force and causes the formation of secondary flow at the beginning of the branch channel (Hager et al., 1987 and 1992, Ferziger et al., 2002, Law et al., 1966). Using numerical models to simulate the flow field decreases the

• Corresponding Author email: sohrab_karimi68@yahoo.com

experimental costs and saves time. Therefore, numerous numerical studies have been conducted on the flow within diversion channels. The three-dimensional flow within intake was simulated using finite volume method in this study (Ramamurthy at al., 1990, Hsu et al., 2002, Chen et al., 1992, Neary et al., 1999).

Soft computing and different artificial intelligence techniques have been widely used for modeling purposes in the recent past decades to predict nonlinear systems and complex problems. Researchers have recently conducted studies on hydrology and hydraulics phenomena in dividing channel using artificial intelligence techniques (Bilhan et al., 2011, Karimi et al., 2015, Kim et al., 2008, Bonakdari et al., 2011, Baghalian et al., 2012, Kashkuli et al., 1964, Ebtehaj et al., 2013, Dursun et al., 2012). However, there is not a lot of documented studies on open channel intake modeling. The main aim of the present study was to predict the mean velocity of the flow within intakes in different width ratios using a neural network. First, 3D flow field of a 90-degree intake was simulated in various width ratios using the ANSIS0CFX software. The experimental model was used to verifying the CFX model. Then, the numerical simulation results were used to design and model an ANN-MLP neural network for predicting the mean velocity in the channel.

2. Methods

2.1. Experimental model

The experimental model of Ramamurthy et al. (2009) was used to verify the results of the numerical simulation. The experimental model was a rectangular horizontal channel attached to a 90-degree weir. The length of the main channel and the weir were 6.198 and 2.794 m, respectively. The width and height of the both channels were constant and equal to 0.61 and 0.305 m, respectively. The intake was located 2.794 m away from the entrance of the main channel. The discharge was equal to $Q_u = 0.046 \frac{m^3}{s}$ at the entrance of the main channel and $Q_b = 0.038 \frac{m^3}{s}$ at the entrance of the branch channel. Moreover, the ratio of the branch channel discharge to the main channel discharge was $Q_r = \frac{Q_b}{Q_u} = 0.838$. The general design of Ramamurthy et al. (2009) main channel and intake is illustrated in "Figure 1".

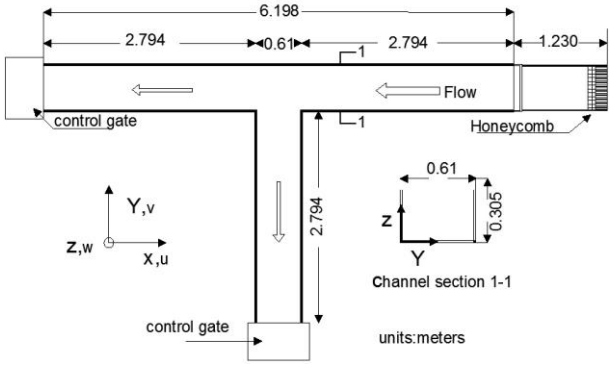

Fig. 1. General design of Ramamurthy et al. (2007) intake used in the present study

All parameters in the extracted results have been made dimensionless through the channel width (b= 0.61 m) and main channel upstream critical velocity (v_c). The critical velocity in the main channel upstream was calculated using $v_c = \left[\frac{\left(Q_u^{\,2}\right)}{gb^2}\right]^{\frac{1}{3}}$ in which Q_u is the discharge of the main channel upstream, b is the main channel width, and g is gravitational acceleration. In addition, the dimensionless coordinate axes were indicated as $x^* = x/b$, $y^* = y/b$ and $z^* = z/b$ and the dimensionless velocities in x, y, and z coordinates were indicated as u^*, v^*, and w^*.

2.2. Numerical model

To conduct the numerical modeling in this study through using ANSYS-CFX software, Navier-Stokes averaged equations and continuity equations should be solved. The two equations are as follows:

$$\frac{\partial \rho}{\partial t} + \frac{\partial}{\partial x}\left(\rho u_j\right) = 0 \quad (1)$$

$$\frac{\partial}{\partial x}\left(\rho u_j\right) + \frac{\partial}{\partial x_j}\left(\rho u_i u_j\right) = \frac{\partial p}{\partial x_i} + \frac{\partial}{\partial x_j}\left[\mu\left(\frac{\partial u_i}{\partial x_j} + \frac{\partial u_j}{\partial x_i} - \frac{2}{3}\delta_{ij}\frac{\partial u_i}{\partial x_j}\right) + \frac{\partial}{\partial x_i}\left(-\rho\overline{u_i'}\overline{u_j'}\right)\right] \quad (2)$$

where u_i and u_j are velocities in x and y directions, respectively, p is the total pressure, ρ is the fluid density and δ_{ij} is Kronecker delta and $\left(-\rho\overline{u_i'}\overline{u_j'}\right)$ is the Reynolds stress.

First, the Reynolds stress must be calculated through turbulence models and then, the momentum equation should be solved (Eq. 2). k-ω turbulence model was used in this simulation. This method is considered as one of the two-equation models of turbulence in which the first turbulence parameter is turbulence kinetic energy (k) and the second turbulence parameter is Specific Dissipation Rate (ω) (Kisi et al., 2012).

The boundary condition of the normal velocity was used in the entrance of the main channel and for the exit boundaries of the field (branch's exit and the main channel) in this study. The boundary conditions of the wall and the floor of the channel wall were assumed to be smooth, and the walls being motionless and was used for a high level of opening boundary condition. Free surface of the flow field was defined and determined according to Eulerian viewpoint. The volume of the fluid (VOF) model was used to define the free surface.

One of the important parameters in speeding up the execution of the model is the regionally suitable reticulation in which the current flows in. To obtain an optimum reticulation, the main channel was divided into three sections. The first section was 2.794 m long and was located in the upstream of the main channel, the second section was 0.61 m long and was located in the middle of the main channel and the third section was 2.794 m long and was located in the downstream of the main channel. The size of the cells upstream and downstream of the main channel was 1 cm× 0.5 cm× 0.5 cm, in the middle section it was 0.5 cm× 0.5 cm× 0.5 cm and the size of the cells of the branch channel network was selected to be 0.5 cm× 0.5 cm× 0.5 cm and the calculations were carried out using these sizes. The numerical results were compared with the experimental results and an acceptable degree of consistency concerning the resulting error percentage was observed. Figure 2 shows the plan and the façade of the calculative field reticulation in the intake.

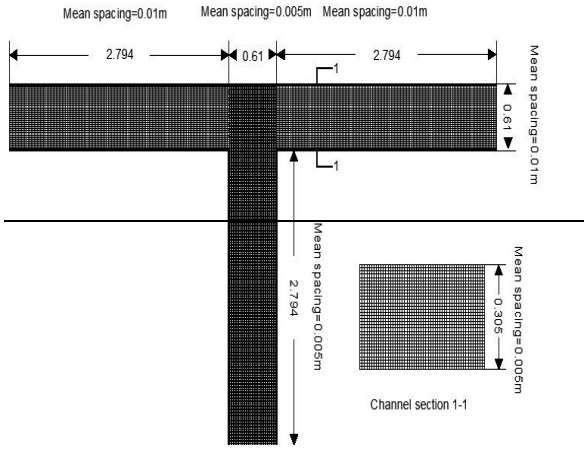

Fig. 2. Plan and façade of the calculative field reticulation in the intake

2.3. Artificial Neural Network

The artificial neural network (ANN) method is considered as one of the soft computing methods. One of the benefits of this method is its desirable performance in analyzing complex flows. In addition, the nonlinear models of flow can also be studied

through this method. The basis of the process in this method is training and learning processes. The components of the ANN structure include hidden layers, hidden units and hidden neurons, the input layer, and output layer (Bilhan et al., 2011, Karimi et al., 2015).

The flexible structure of the artificial neural network makes it capable of modeling complex and nonlinear patterns between input and output data. The capability to estimate the accurate results is achieved through using input data on the basis of training and learning the process. What is meant by training the neural network is to obtain the weights (w) of the network. In addition, classifying different types of ANN is done based on the methods of obtaining the weights and also the utilized transfer functions. One of the various types of neural network that is used frecuentely is Multilayer Perceptron (MLP). An MLP feed forward includes an input layer, one or more hidden layers and an output layer (Fig. 3). Each layer is made up of some neurons the number of which in the input and output layers is equal to the number of inputs and outputs of the under-study issue, respectively. Various types of functions could be considered as sigmoid function. Hyperbolic tangent was used as the activation function in the hidden layers in this study. Levenberg-Marquardt method was used for training ANN. Back-propagation algorithm, which is one of the most beneficial algorithms, was used in order to figure out the weights and bias of the neural network in this method. This algorithm minimizes the difference between the observed outputs from the laboratory studies and the ANN model outputs very quickly through determining weights and bias (Smith, 1993).

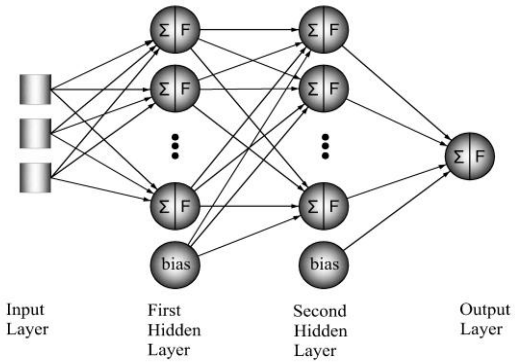

Fig. 3. General view of ANN-MLP

The modeling and simulation of ANN-Multilayer Perceptron (MLP) was written by the Matlab programming language in this study. In order to analyze and solve a neural network that has two hidden layers and in order to determine the number of the existing neurons in each layer, trial and error method was used. The functions and equations that are analyzed for the output layer are linear (Kisi et al., 2012, Melesse et al., 2011, Smith, 1993). The way the trial and error method works is that various runs are taken in order to determine the number of neurons of the layers of the neural network in case the number of the neurons are not equal in the first and the second layer. Then the RMSE error is determined for each of them separately and the state that has the least amount of error will be selected as the base for modeling ANN. In this study, three data were considered as input and one data was considered as output. The used input parameters in this study were dimensionless and the inputs include nondimentionalized coordinates (y^*), the ratio of the width of the subsidiary channel to the width of the main channel (w_r) and the linear mean velocity (v^*_{line}), which presents the read velocities on the CFD model and present the mean velocity on the middle line of the branch channel. These parameters were placed in the first layer of the neural network

as the input parameters. The neural network was trained through a number of these parameters within the middle layer in the following stage so that they could gain their optimum structure and after reaching the already determined stopping point, the training process stopped. As mentioned earlier, the purpose of the structured neural network is to estimate the real average speed within the channel, therefore the neural network used in this study predicted the real average velocity of the surface in which the flow meter was located in through the aid of y^*, w_r, and v^*_{line}.

3. Results

The experimental model by Ramamurthy et al. (2009) was simulated three-dimensionally in two phases of air and water in this section using ANSYS-CFX model. In order to verify the CFX model, the results of the numerical model were compared with the experimental results. The numerical model was simulated for different widths after verifying the CFX model and the v^*_{line} mean velocity was calculated afterwards in the vertical column in the center of the branch channel at different heights. Then the real mean velocity of the flow in the branch channel was extracted from the results of the CFD model in the areas with no experimental data. An ANN-MLP neural network was then designed and modeled using the results of the numerical simulation. Coordinates (y^*), the ratio of the branch channel width to the main channel width (w_r) and the linear mean velocity V^*_{line} dimensionless parameters were selected as the input data entering the ANN-MLP neural network for this purpose. The results obtained from the neural network were compared with the mean velocity in the weir in order to examine the accuracy of ANN-MLP model.

3.1 CFX Model validity

In order to validate the results of the CFX model, v^* (dimensionless velocity) of the numerical and experimental models in the channel was compared (Fig. 4). v^* values are shown in this figure for x^* values of -0.1, -0.328, -0.558, and -0.787 in $Q_r = \frac{Q_b}{Q_u} = 0.838$. Two statistical indexes were used to validate the results of the CFX model including the Root Mean Square Error (RMSE) and Mean Absolute Percentage Error (MAPE) defined as follows.

$$\mathrm{RMSE} = \sqrt{\left(\frac{1}{n}\right)\sum_{i=1}^{n}\left(v_{\mathrm{EXP_i}} - v_{CFD_i}\right)^2} \qquad (3)$$

$$\mathrm{MAPE} = \left(\frac{1}{n}\right)\sum_{i=1}^{n}\left(\frac{\left|v_{\mathrm{EXP_i}} - v_{CFD_i}\right|}{v_{\mathrm{EXP_i}}}\right)\times 100 \qquad (4)$$

Where $v_{\mathrm{EXP_i}}$ denote the experimental velocity and v_{CFD_i} denote the velocity results of CFD model, respectively. (RMSE) index presents the second root of the squared error and explains the difference between the numerical and experimental values and considers larger error weights. MAPE index presents the difference between the experimental and CFX model in the form of a percentage of real values.

Table 1 shows the statistical indexes obtained for the results of CFX model and the experimental model for different Y^* cross sections.

Table 1- Statistical Indexes

	Y*= -0.29	**Y*= -1.0**	**Y*= -1.69**
RMSE	0.01	0.012	0.017
MAPE (%)	2	5.2	6.95

MAPE's average relative error was approximately 2%, 5.2%, and 6.95% in three cross sections of y^*= -0.29, -1.0, -1.62, respectively, which is an indication of conformity between the CFX model and the experimental model results (Table 1). RMSE index is used for the purposes of quantitative examination of models. The table shows that the RMSE for y^*= -0.29, -1.0, -1.62 cross sections was 0.01, 0.012 and 0.017, respectively. Taking into consideration the results of verification, it can be seen that the results of the CFX model are slightly different from the results of the experimental model in the branch channel downstream y^*= -1.0 and 1.62. Despite that, the maximum MAPE error obtained was equal to 6.95% that indicates the CFX model is fairly accurate. Because of this difference in the separation zone, and the contraction zone since the v^* decreases in the separation zone due to the presence of the recirculation zone and therefore, v^* becomes negative. v^* was maximum in the contraction zone and depths of z^*= 0.0 to 0.2 and the contraction zone was denser in this area in comparison with the flow surface.

3.2 ANN prediction of mean velocity in the intake

The neural network produced in this study had two hidden layers with an unknown number of nodes. Therefore, the number of the hidden nodes was determined through "trial and error" in the process of solving and analyzing using the neural network model. The number of the hidden nodes is constantly changing in trial and error, and an RMSE amount obtained for each of the hidden nodes. RMSE was used to obtain the error unique to each hidden node in the present neural network. Each hidden node that had the minimum RMSE amount was determined as the chosen node. The minimum amount of RMSE obtained for the designed ANN model was equal to 6.36E-0.5 and this error was related to the state where there were 7 neurons within the first layers and 5 neurons within the second layer. Therefore, this state was selected as the base of the neural network. The geometric and algorithm views of the obtained neural network are shown in Fig. 5.

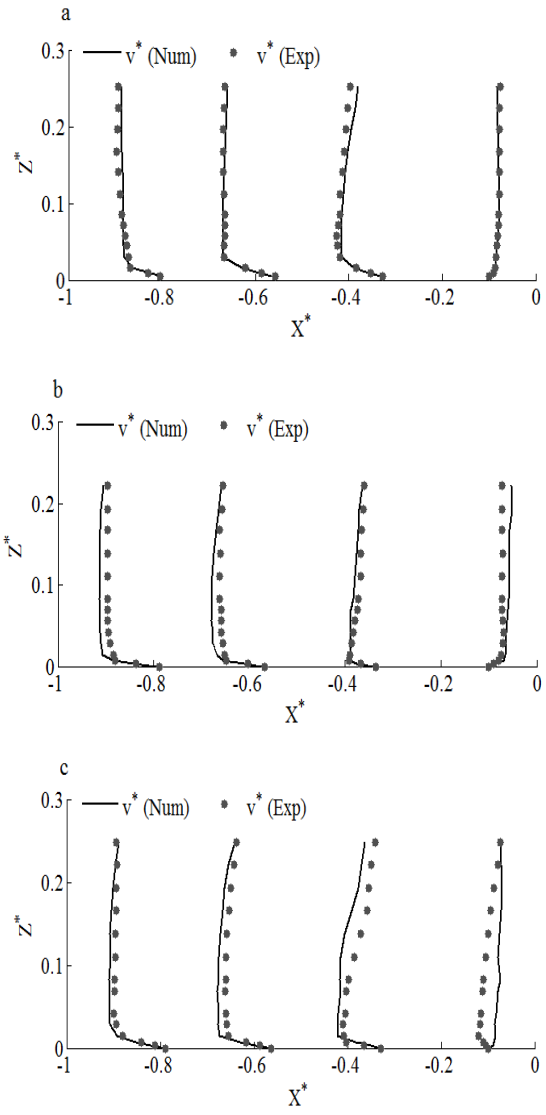

Fig. 4. Verification graphs between the CFX model and Ramamurthy et al.'s (2007) experimental model results in: a) y*=-0.29, b) y*=-1.00 and c) y*=-1.62

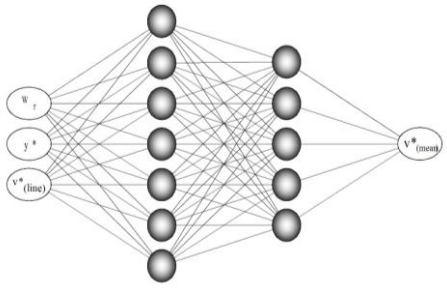

Fig. 5. The algorithm of the optimum ANN neural network

The major objective of presenting the ANN-MLP neural network model was to predict the mean velocity within the weir. In order to qualitatively examine the predicted amounts in the "test" state, the results of ANN-MLP model have been shown as scattered plot in width ratios of 1.4, 1.2, 1, 0.8, and 0.6 in Fig. 6. The vertical coordinate presents the v^* in ANN-MLP model, and the horizontal coordinate represents the v^* observed in the experimental model. The line equation with $y=C_{1X}+C_2$ was used in the scatter plot. C_1 and C_2 are constants for evaluating the accuracy of the model. The closer C_1 is to 1, and the closer C_2 is to zero, the more accurate is the ANN-MLP model. Considering Fig. 6, the ANN-MLP model is most accurate in the width ratio of 1.2 in comparison with the other width ratios since in this width ratio, the line equation with $y=C_{1X}+C_2$ has the maximum C_1 equal to 0.9964 and the minimum C_2 equal to 0.00005. Determination coefficient value (R^2) is another index for examining the accuracy of the ANN-MLP model that indicates the linear correlation between the predicted and experimental amounts. The closer R^2 to 1, the more accurate is the ANN-MLP model. Therefore, taking into account Fig. 6, the ANN-MLP model has the maximum (R^2) in the width ratio of 1.2, which is equal to 0.9822. Therefore, it is the most accurate in predicting the mean velocity in the channel. When the linear fit line is located on the left side and on the right side of the exact line, the presented model is being overestimated and underestimated, respectively. It could be seen in Fig. 7 that the ANN-MLP model has been underestimated in the width ratio of 1, but in the width ratios of 1.4, 1.2, 0.8, and 0.6, the linear fit line was almost on the exact line. Therefore, it could be concluded that the ANN-MLP model is least accurate in the width ratio of 1, and this is due to the vastness of the separation zone and the contraction zone in this width ratio.

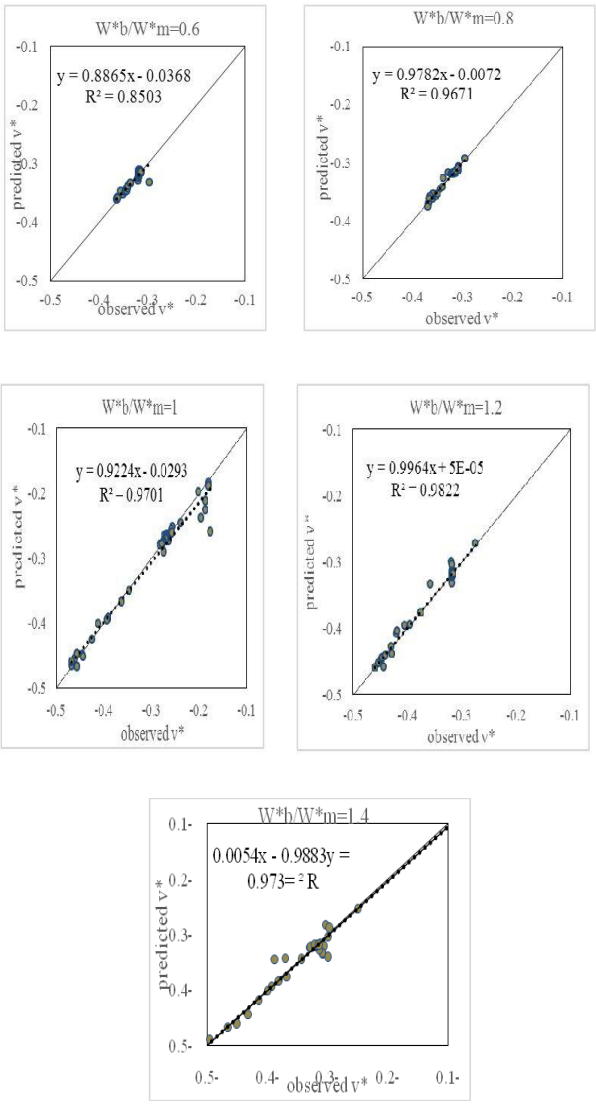

Fig. 6. Difference between the predicted average velocity by the neural network and the real average velocity in the channel for different width ratios

The predicted results are presented in Fig. 7 in the training state. The *x*-axis of this figure indicates the predicted velocity in the weir channel and the *y*-axis represents the experimental velocity. The little square in the figure indicates the amount of V^*_{mean} predicted by the ANN-MLP model, and the filled-in circles indicate the observed V^*_{mean} in the experimental model. According to this figure, the estimated values by the ANN-MLP model fairly conform to the experimental ones.

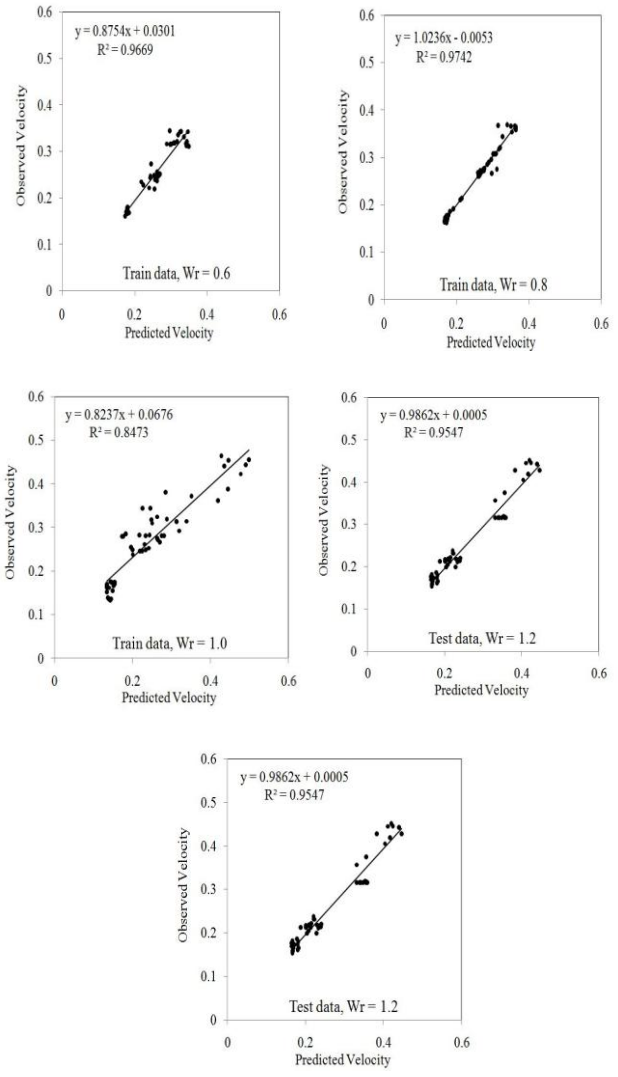

Fig. 7. Comparison of the predicted and experimental V^*_{mean} in testing state

4. Conclusions

One of the strategies used to prevent flood and deviate flow in the irrigation networks and drainage systems is utilizing intakes. Calculating the mean velocity of the flow is amongst the most crucial hydraulic parameters in increasing the intake efficiency. The main aim of this research was to present an applicable solution for predicting the real mean velocity taking into consideration the velocity obtained from the numerical models in confluence zone in the open channel. The verification error percentage mean was approximately 5%, and RMSE of simulation was 0.013, which indicated that the results of the ANSYS-CFX modeling fairly conform to the experimental data. Soft computing was used to predict the real mean velocity within the branch channel better and more accurately. Moreover, the method presented is ANN-MLP method that predicts the real mean velocity within the channel through receiving coordinates (y^*), the ratio of the branch channel width to the main channel width (w_r) and the linear mean velocity parameters (V^*_{line}), which were obtained by the numerical model. The results show that combining the flowmeter measurements and the ANN-MLP method could simulate the mean velocity of intake flow with a mean R^2 value of 0.948. Taking into consideration that there is a relatively slight difference between the real mean velocity and the mean velocity extracted through the ANN-MLP model in all width ratios it becomes clear that the presented neural network has a proper level of accuracy in predicting the mean velocity within a branch channel.

Nomenclature

b	main channel width
g	Acceleration Gravity
$\rho\overline{U'iU'j}$	Reynolds stress
Y^*	longitudinal coordinates
P	The total pressure
ρ	fluid density
k	turbulence kinetic energy
ω	Specific Dissipation Rate of the second turbulence
β', α, , σ_k,σ_ω	constant assume the standard values
P_k	Production rate of turbulence
Q_u	the main channel upstream discharge
Q_b	the branch channel discharge
x^*	branch channel width
z^*	water depth
Re	Reynolds number
u^*	No dimensional velocity at x axis
U	longitudinal velocity in x axis
V_c	critical velocity of main channel upstream
V	longitudinal velocities at y axis
V_{line}	average velocity in the vertical column of the branch channel
W_r	the ratio of channel width to the main channel width

References

Seyediyan and Shafai Bejestan, (1389), Suspended sediments entered the intake with two side wall angles of 90-degree and 45-degree. J. of Water and Soil, ferdousi Uni. Of Mashhad, 985-994.

Shamlou and Pirzadeh, (1389), Effects of Geometric and Hydraulic parameters on the dimensions of the flow separation zone of the lateral intakes using Fluent. J. of Civil Eng.-Mapping, Tehran Uni.

Safarzadeh and Salehi Neyshabouri, (1387), Hydrodynamic study of the turbulent flow pattern and sediment transfer in the Karoun River using a 2D numerical model, 3rd Conference of Water Resource Management, Tabriz Uni.

Safarzadeh and Salehi Neyshabouri, (1383), 3D Numerical Modeling of the flow pattern in the lateral intake. 1st national congress of Civil Eng., Sanati Sharif Uni.

Ramamurthy, A. Qu, J., Vo, D., (2007), Numerical and experimental study of dividing open-channel flows. Journal of Hydraulic Engineering, 133(10), 1135-1144.

Issa, R. I., Oliveira. P. J., (1994), Numerical prediction of phase separation in two-phase flow through T-junction, Comp. and Fluids, 23(2), 347-356.

Neary, V. S., Sotiropoulos, F., (1996), Numerical investigation of laminar flows through 90-degree diversions of rectangular cross section. Computational and Fluids, 25(2), 95-118.

Shettar, A. S., and Murthy, K. K., (1996), A numerical study of division of flow in open channels. Journal of Hydraulic Research, 34(5), 651-675.

Barkdoll, B. D., Hagen, B. L., Odgaard, A. J., (1998), Experimental comparison of dividing open-channel with duct flow in T-junction. Journal of Hydraulic Engineering, 124(1), 92-95.

Hager, W. H., (1987). Discussion of Separation Zone at Open-Channel Junctions by James L. Best and Ian Reid (November, 1984). Journal of Hydraulic Engineering, 113(4), 539-543.

Hager, W. H., (1992), Discussion of 'Dividing flow in open channels' by A. S. Ramamurthy, D. M. Tran, and L. B. Carballada. J. Hydraul. Eng., 118(4), 634-637.

Ferziger, J. H., and Peric, M., (2002), Computational method for fluid dynamics, 3rd Ed., Springer, New York.

Law, S.W. and Reynolds, A. J., (1966), Dividing flow in an open Channel. Journal of Hydraulic Div. 92(2), 4730-4736.

Ramamurthy, A. S., Tran, D. M., and Carballada, L. B., (1990), Dividing flow in open channels. J. Hydraul. Eng., 116(3), 449-455.

Hsu, C. C., Tang, C. J., Lee, W. J., and Shieh, M. Y., (2002), Subcritical 90° equal-width open-channel dividing flow. J. Hydraul. Eng., 128(7), 716-720.

Chen, H. B., and Lian, G. S., (1992), The numerical computation of turbulent flow in T-junction. J. Hydrodynamics, 3, 16-25, 50-58.

Neary V. S., Odgaard A., Sotiropoulos F., (1999), Three-dimensional numerical model of lateral-intake inflows. Journal of Hydraulic Engineering, 125(2), 126-140.

Bilhan, O., Emiroglu, M. E., Kisi, O., (2011), Use of artificial neural networks for prediction of discharge coefficient of triangular labyrinth intake in curved channels. Advances in Engineering Software, 42(4), 208-214.

Karimi, S., Bonakdari, H., and Gholami, A., (2015), Determination Discharge Capacity of Triangular Labyrinth Side Weir using Multi-Layer Neural Network (ANN-MLP), Special Issue of Curr. World Environ., 10 (Special Issue May 2015). Available from: http://www.cwejournal.org/?p=10430

Kim, B, Lee, S. E., Song, M. Y., Choi, J. H., Ahn S. M., and Lee, K. S., (2008), Implementation of artificial neural networks (ANNs) to analysis of inter-taxa communities of benthic microorganisms and macro invertebrates in a polluted stream. Sci. Total Environ, 390, 262-274.

Bonakdari, H., Baghalian, S., Nazari, F., Fazli, M., (2011), Numerical analysis and prediction of the velocity field in curved open channel using Artificial Neural Network and Genetic Algorithm. Engineering Application of Computational Fluid Mechanics, 5(3), 384-396.

Baghalian, S., Bonakdari, H., Nazari, F., Fazli, M., (2012), Closed-form solution for flow field in curved channels in comparison with experimental and numerical analyses and Artificial Neural Network. Engineering Application of Computational Fluid Mechanics, 6(4), 514-526.

Kashkuli, H. A., (1964), A numerical linked model for the prediction of the decline of ground water models.

Ebtehaj, I., Bonakdari, H., (2013), Evaluation of Sediment Transport in Sewer using Artificial Neural Network. Engineering Applications of Computational Fluid Mechanics, 7(3), 382-392.

Dursun, O. F., Kaya, N., Firat, M., (2012), Estimating discharge coefficient of semi-elliptical intake using ANFIS. Journal of Hydrology, 426, 55-62.

Kisi, O., Emiroglu, M. E., Bilhan, O., Guven, A., (2012), Prediction of lateral outflow over triangular labyrinth intake under subcritical conditions using soft computing approaches. Expert Systems with Applications, 39, 3454-3460.

Melesse, A., S. Ahmad, M. McClain, X. Wang and Y, Lim., (2011), Suspended sediment load prediction of river systems: An artificial neural network approach. Agricultural Water Management 98(5), 855-866.

Smith, M., (1993), Neural networks for statistical modeling, Thomson Learning.